HST WFPC2 OBSERVATIONS OF MARS SURFACE MINERALOGY AND ATMOSPHERIC CONDENSATES; J. F. Bell III, A. E. Switala (Cornell University, Ithaca NY), D. Crisp (JPL/Caltech, Pasadena CA), and the WFPC2 Science Team

We used the Hubble Space Telescope (HST) Wide Field/Planetary Camera-2 (WFPC2) to take images of Mars on UT 23-26 February and 11 April 1995, just after opposition. Mars was imaged using the Planetary Camera and discrete filters at ultraviolet (160, 255, 336 nm) and near infrared (1042 nm) wavelengths to place improved constraints on the airborne dust and ice optical depths and the ozone column abundances. These images are also being used to produce high-spatial resolution maps of the surface CO_2 and H_2O frost deposits and other surface albedo features. We also imaged Mars using the WFPC2's Linear Ramp Filter (LRF) in order to spatially map variations in the surface and dust ferric and ferrous iron mineralogy. The LRF is a continuously variable narrowband filter that allows 1.25% spectral resolution images to be obtained at nearly any wavelength between 370 and 980 nm. An HST command interpretation error prevented us from obtaining the exact LRF wavelengths that we requested; however, LRF images were obtained at 565, 619, 640, 724, 850, 870, 889, and 918 nm. The characteristics of our entire 1995 Mars opposition data set are listed in Table 1.

Table 1. Characteristics of the 1995 WFPC2 Team HST Mars Data Set

Image #	Date (UT)	Time (UT)	SE Lon (°)	Filter Chip/Name	Mean λ (nm)	Image #	Date (UT)	Time (UT)	SE Lon (°)	Filter Chip/Name	Mean λ (nm)
1	950223	1151	207.3	WF4/FR680N	724[a]	25	950226	0106	23.7	PC1/F1042M	1018
2	950223	1157	208.8	WF4/FR868N	850	26	950226	0112	25.1	WF4/FR533N	565[a]
3	950223	1215	213.2	WF2/FR868N	918	27	950226	0117	26.4	WF2/FR680N	619[b]
4	950223	1220	214.4	WF3/FR868N	870[c]	28	950226	0123	27.8	WF3/FR680N	640[a]
5	950223	1226	215.8	WF3/FR868N	889[c]	29	950226	0233	44.9	WF4/FR680N	724[a]
6	950223	1326	230.5	PC1/F336W	334	30	950226	0238	46.1	WF4/FR868N	851
7	950223	1329	231.2	PC1/F255W	259	31	950226	0256	50.5	WF2/FR868N	918
8	950223	1334	232.4	PC1/F1042M	1018	32	950226	0302	52.0	WF3/FR868N	870[c]
9	950223	1339	233.6	WF4/FR533N	565[a]	33	950226	0307	53.2	WF3/FR868N	889[c]
10	950223	1345	235.1	WF2/FR680N	619[b]	34	950226	0552	93.4	PC1/F336W	334
11	950223	1350	236.3	WF3/FR680N	640[a]	35	950226	0555	94.1	PC1/F255W	259
12	950225	1833	287.8	WF4/FR680N	724[a]	36	950226	0600	95.4	PC1/F1042M	1018
13	950225	1838	289.0	WF4/FR868N	851	37	950226	0605	96.6	WF4/FR533N	565[a]
14	950225	1856	293.4	WF2/FR868N	918	38	950226	0611	98.0	WF2/FR680N	619[b]
15	950225	1901	294.7	WF3/FR868N	870[c]	39	950226	0616	99.3	WF3/FR680N	640[a]
16	950225	1907	296.1	WF3/FR868N	889[c]	40	950226	0724	115.9	WF4/FR680N	724[a]
17	950225	2007	310.7	PC1/F336W	334	41	950226	0730	117.3	WF4/FR868N	851
18	950225	2010	311.5	PC1/F255W	259	42	950226	0900	139.3	WF2/FR868N	918
19	950225	2015	312.7	PC1/F1042M	1018	43	950226	0906	140.8	WF3/FR868N	869[c]
20	950225	2020	313.9	WF4/FR533N	565[a]	44	950226	0911	142.0	WF3/FR868N	889[c]
21	950225	2026	315.4	WF2/FR680N	619[b]	45	950411	0205	0.0	WF3/F336W	337
22	950225	2032	316.8	WF3/FR680N	640[a]	46	950411	0213	2.0	WF3/F160BN15	147
23	950226	0058	21.7	PC1/F336W	334	47	950411	0233	6.8	WF3/F336W	337
24	950226	0101	22.5	PC1/F255W	259	48	950411	0343	23.9	WF3/F160BN15	147
						49	950411	0502	43.1	WF3/F160BN15	147

[a]Wavelength resolution degraded by mixing between two LRF segments
[b]Most pixels in image are saturated
[c]Image is partially vignetted

The February HST Mars images were taken at 4 sub-earth longitudes (~22, 94, 231, and 311 degrees) to provide near-global coverage with a minimum of foreshortening. Examples of images obtained at 1042 nm are shown in Figure 1. The images were obtained with different scientific goals than previously-obtained HST Mars images [e.g., 1-3]. However, this data set extends and augments the previous and ongoing HST imaging programs by providing additional diurnal and seasonal coverage of variable Martian surface and atmospheric features and by providing a set of multispectral images specifically focused on surface and airborne dust mineralogy.

The raw images were processed using standard HST data reduction procedures. The steps included correction for analog-to-digital conversion errors, subtraction of bias, superbias, and superdark frames, correction for shutter shading effects, flatfielding, correction for charge transfer efficiency variations, and correction of bad pixels and cosmic ray hits. Because we were the first

users of the LRF on HST, these processes were supplemented by special flatfielding procedures developed because the proper on-orbit LRF calibration frames had not yet been obtained. No correction has yet been performed for the well-characterized point spread function of WFPC2, and the images have not yet been calibrated to an absolute flux scale. Both of these last steps will be attempted in the near future.

The near-ultraviolet images at 255 and 336 nm reveal a dark Martian surface with a bright north polar cap and bright water ice clouds (Figure 2). The ice clouds are concentrated near the morning and evening limbs and at latitudes south of 50 degrees, forming a south polar hood. A few discrete bright clouds were also seen near the Tharsis volcanoes and over Elysium Mons. The morning limb was in shadow at the surface, but the atmosphere was still illuminated at altitudes above ~25 km. The clouds near the morning limb are confined below this altitude. In contrast, there is a high-altitude detached haze layer on the evening limb. The south polar hood is much darker at 255 nm than at 336 nm. This darkening has been attributed to enhanced ozone absorption at these latitudes.

The 1042 nm images reveal the well-known bright and dark albedo markings (Figure 1). The surface and atmospheric ices are much less apparent at this wavelength. For example, the north polar cap is only 75% as bright as the brightest regions of Elysium. The relatively bright, red, airborne dust is more easily detected, however. The largest dust optical depths are seen over the relatively dark, heavily-cratered terrain just south of the equator.

The images have been map-projected and assembled into a 3-dimensional image cube in order to allow for the extraction of spectra of individual surface units and to allow the production of ratio images and band depth maps [4]. Based on laboratory reflectance spectra convolved and resampled to the wavelengths of this HST data set, we conclude that the combination of LRF wavelengths and PC filters will allow for the detection and mapping of a number of ferric and ferrous minerals with relevance to Mars.

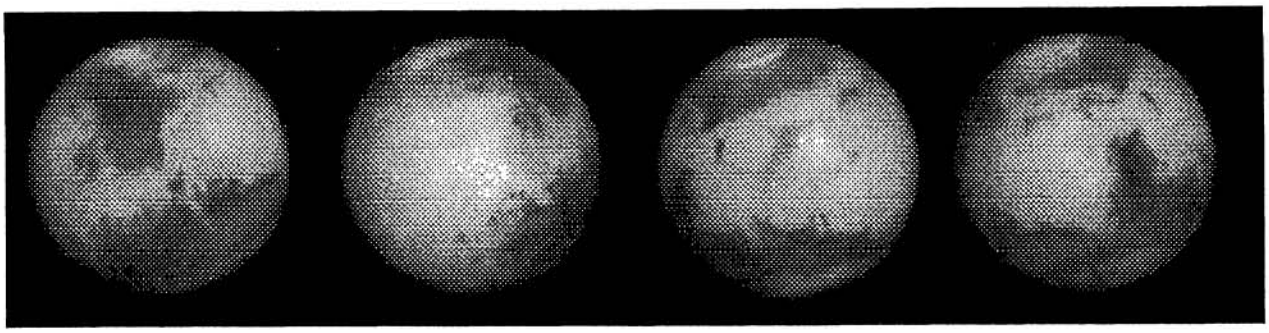

FIGURE 1: Four views of Mars obtained at 1042 nm by HST on February 23-26, 1995.

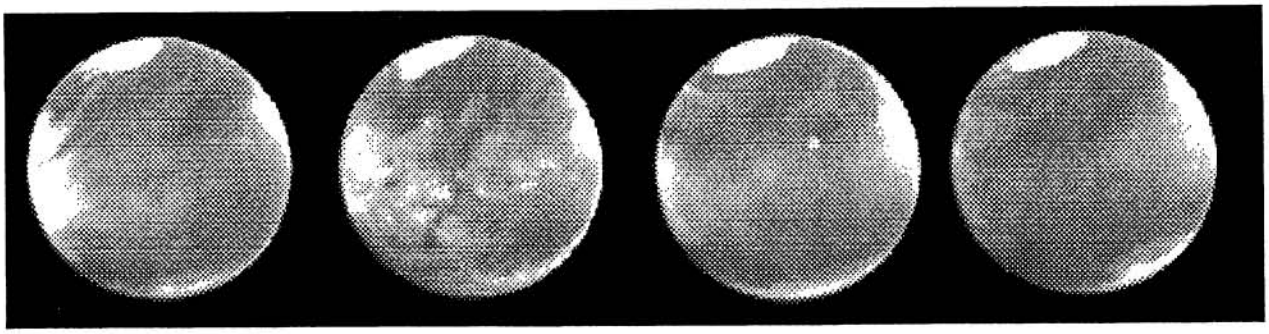

FIGURE 2: Same views as Fig. 1 but at 336 nm. HST data from February 23-26, 1995.

REFERENCES: [1] James, P.B. *et al.* (1994) *Icarus 109*, 79-101. [2] Bell, J.F. III *et al.* (1995) *LPSC XXVI*, 95. [3] James, P.B. *et al.*, (1995) LPI Tech. Rpt. 95-04, 16-17. [4] Bell, J.F. III and D. Crisp (1993) *Icarus, 104,* 2-19.